AIP Journal of Applied Physics

Design considerations for surface plasmon resonance based detection of human blood group in near infrared

Anuj K. Sharma, Rajan Jha, and Himansu S. Pattanaik

Citation: Journal of Applied Physics **107**, 034701 (2010); doi: 10.1063/1.3298503
View online: http://dx.doi.org/10.1063/1.3298503
View Table of Contents: http://scitation.aip.org/content/aip/journal/jap/107/3?ver=pdfcov
Published by the AIP Publishing

Design considerations for surface plasmon resonance based detection of human blood group in near infrared

Anuj K. Sharma,[1,a)] Rajan Jha,[2] and Himansu S. Pattanaik[3]
[1]*Jacob Ruisdaellaan 3, 5581 JK Waalre, The Netherlands*
[2]*School of Basic Sciences, Indian Institute of Technology Bhubaneswar, Samantapuri, Bhubaneswar 751013, India*
[3]*3039 White Ash Trail, Orlando, Florida 32826, USA*

(Received 17 November 2009; accepted 2 January 2010; published online 5 February 2010)

Surface plasmon resonance based sensor for detection of different human blood groups in near infrared region is proposed. The plasmonic structure is based on fused silica or chalcogenide sulfide glass $Ge_{20}Ga_5Sb_{10}S_{65}$, commonly known as 2S2G. Experimental results describing the wavelength-dependent refractive index variation in multiple samples of different blood groups are considered for theoretical calculations. The angular interrogation method is considered. The sensor's performance is closely analyzed in terms of its angular shift and curve width in order to predict the design consideration for simple and accurate blood-group identifier. The results are explained in terms of light coupling and plasmon resonance condition. Chalcogenide glass-based SPR structure is able to provide highly precise detection of different blood groups. The proposed low-volume blood sensor can be very useful for simple and reliable blood sample detection in medical application. © *2010 American Institute of Physics*. [doi:10.1063/1.3298503]

I. INTRODUCTION

Since past two decades, surface plasmon resonance (SPR) has become a powerful conceptual tool for sensing a wide range of biological,[1–3] physical,[4,5] and chemical[6,7] parameters and phenomena. The SPR sensing principle is an optical phenomenon in which a *p*-polarized light beam satisfies the certain resonance condition and excites a charge density oscillation [known as surface plasmon wave, (SPW)] propagating along the metal-dielectric interface. The plasmon resonance condition is expressed as

$$K_0 n_c \sin\theta_{\mathrm{SPR}} = K_0 \left(\frac{\varepsilon_{mr} n_s^2}{\varepsilon_{mr} + n_s^2} \right)^{1/2}. \quad (1)$$

The term on left hand side is the propagation constant (K_{inc}) of a light beam incident at a resonance angle θ_{SPR} through the light coupling device of refractive index n_c. The right hand term is SPW propagation constant (K_{SP}) with ε_{mr} being real part of the metal dielectric constant (ε_m) and n_s as the refractive index of sensing (dielectric) medium. When the above condition is fulfilled, the resonance appears in the form of a sharp dip of output optical signal at resonance value (θ_{SPR}) of incident angle [Fig. 1(a)]. Any change in refractive index near the metal-dielectric interface causes a shift in the value of resonance angle (as is shown in Fig. 1(a) with another dotted curve). In general, the performance of any SPR sensor is determined in terms of two aspects. First is the sensitivity aspect which means that the shift in resonance angle ($\delta\theta_{\mathrm{SPR}}$) for a given change ($\delta n_s$) in sensing layer refractive index should be as large as possible. Second is the accuracy aspect implying that the full width at half maximum (FWHM) corresponding to SPR curves should be as small as possible so that the error in determining the resonance angle is minimum. Hence, detection accuracy of SPR-based sensor can be assumed as inversely proportional to FWHM of SPR curve.

Among the several SPR sensing structures, the most prominent is the Krestschmann attenuated total reflection (ATR) configuration[8] in which a thin metallic layer (typically a few tens of nanometer) is deposited directly on the base of a prism or a glass substrate [Fig. 1(b)]. In the above configuration, it is important that the refractive index of glass substrate [i.e., n_c in Eq. (1)] should be greater than that of sensing medium [i.e., n_s in Eq. (1)]. There will be no coupling of light, and hence no plasmon resonance, if $n_c < n_s$. In general, silica substrates (with refractive index in the vicinity of 1.4) are used for SPR sensing applications. However, it is found that silica-based SPR sensing structures are more effective in visible wavelength region and becomes inapplicable in infrared (IR) and far-IR wavelength ranges. Due to an ever-growing number of sensing applications in whole IR wavelength region, new materials other than conventional ones are required. Recently, chalcogenide glass substrates (with refractive index in the vicinity of 2.2) have been investigated in much detail.[9,10] As a step further, chalcogenide-based SPR sensors with enhanced performance have been presented in recent times.[11,12] Further, the metallic layer that is mostly used in SPR measurements consists of either silver or gold. Silver displays a narrower resonance curve (i.e., smaller FWHM) causing a higher detection accuracy of SPR sensor, but has a poor chemical stability. The oxidation of silver happens as soon as exposed to air or a liquid, which makes silver not-so-suitable candidate to get a reliable SPR sensor for practical applications. Gold, on the other hand, demonstrates a higher shift in resonance angle (i.e., $\delta\theta_{\mathrm{SPR}}$) corre-

a)Author to whom correspondence should be addressed. Present address: ASML Netherlands B.V., P.O. Box 324, 5500 AH, Veldhoven, The Netherlands. Electronic mail: anujsharma@gmail.com.

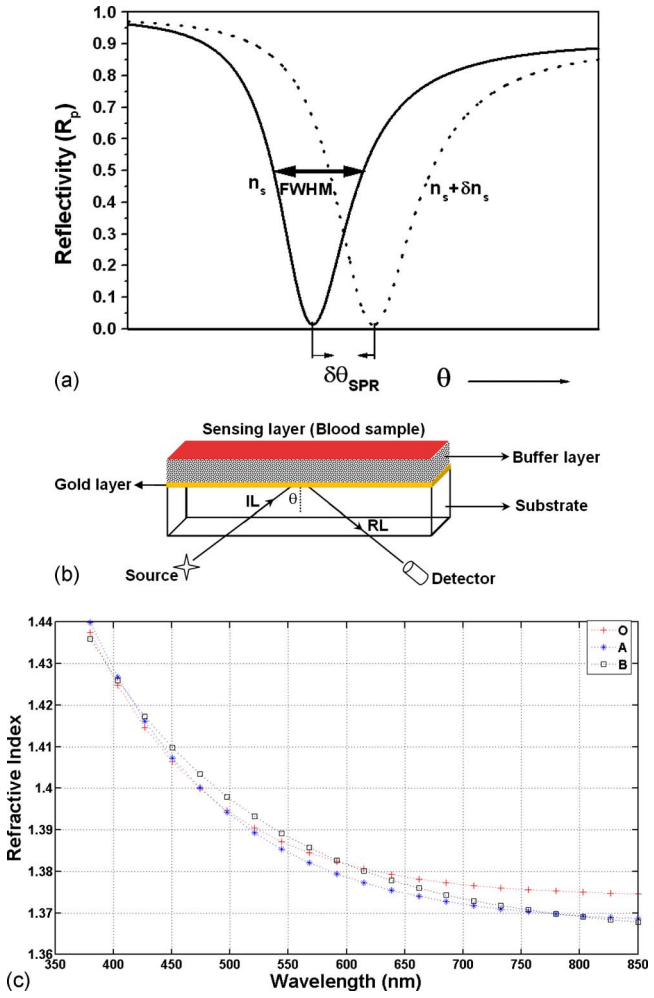

FIG. 1. (Color online) (a) Ilustration of SPR curves for two different sensing media. Shift in resonance angle and FWHM are also illustrated. (b) Proposed SPR setup for the detection of human blood group. (c) Plot for dispersion (refractive index vs wavelength) of samples corresponding to three different blood groups.

sponding to any change in refractive index of sensing layer and is chemically much more stable than silver.

Among various biological parameters, SPR related sensing procedure has been reported for the detection of pesticides, immunoassays, DNA, RNA, and allergens. However, SPR can also be a potential candidate for an efficient detection of blood group of a human blood sample. The logic behind this reasoning is that the different blood groups have different dispersion relationship (i.e., variation in refractive index with wavelength) due to their different chemical and biological compositions. It means that at any operating wavelength, different blood groups should have different values of refractive index. Therefore, in view of Eq. (1), plasmon resonance condition should be satisfied at different resonance angles for different blood groups thereby making it possible to realize a simple, precise and reliable SPR sensing of blood groups.

Li *et al.*[13] experimentally measured the refractive dispersion of three blood groups (O, A, and B) at visible and near IR wavelengths (380–860 nm) for a number of blood samples taken from different healthy donors. Based on their experimental results, they described the refractive dispersion for three blood groups in the form of a Cauchy formula given as

$$n(\lambda) = 1.357 + \frac{A}{\lambda^2} + \frac{B}{\lambda^4}. \tag{2}$$

In the above expression, wavelength (λ) is in nanometer. The Cauchy coefficients may have different values for different blood groups. Based on the fitting of data points of experimental dispersion curves reported by Li *et al.*,[9] Fig. 1(c) shows the variation in refractive index for three different blood groups (O, A, and B) with wavelength. As is apparent, the trend of the curves (i.e., decrease in refractive index with an increase in wavelength) are in accordance with the normal dispersion shown by most of the SPR-active liquid media (e.g., water etc.), which gives a first-hand indication that the SPR sensing can be made possible for blood samples also. The data corresponding to the plots shown in above figure has been used for simulation in the present work.

The present state-of-the-art suggests that despite being highly used for almost three decades, SPR sensing principle is still unexplored for the detection of human blood groups. Therefore, in the present work, we have explored the possibility of designing a SPR-based blood-group sensor by making use of the experimental data provided by Li *et al.*[9] for refractive dispersion of three different blood groups. We report the design considerations to enable a simple, precise, and reliable SPR-based detection of different blood groups. Further, the application of 2S2G Chalcogenide glass for the proposed scheme has also been investigated. The metal layer is taken as a thin gold layer of 50 nm. The angular interrogation method of SPR sensing is used. The sensor's performance is evaluated separately for 2S2G glass-based and silica-based SPR configurations in order to find out the best possible conditions for a highly accurate and reliable SPR-based detection of different blood groups.

II. THEORETICAL MODEL

In this section, we discuss the different constituents of our sensor design along with their optical and other properties.

A. Glass substrate

Under the Kretschmann ATR configuration for the present structure, the coupling device is considered as a bulk glass substrate of refractive index (n_c), which is fused silica for most of the SPR-based applications. The refractive index of fused silica is wavelength dependent and is represented in terms of Sellmeier expression as follows:

$$n_{SiO_2}(\lambda) = \sqrt{1 + \frac{A_1\lambda^2}{\lambda^2 - B_1^2} + \frac{A_2\lambda^2}{\lambda^2 - B_2^2} + \frac{A_3\lambda^2}{\lambda^2 - B_3^2}}, \tag{3}$$

where λ denotes the wavelength (in μm). The coefficients A_1, A_2, A_3, B_1, B_2, and B_3 are known as Sellmeier coefficients and have different numeric values for different materials. The Sellmeier equation for a material describes the dispersion of light in that medium. The Sellmeier coefficients

TABLE I. Sellmeier coefficients to calculate the refractive index of fused silica with Eq. (3).

Sellmeier coefficient	Numeric value
A_1	0.696 166 3
A_2	0.877 479 4
A_3	0.407 942 6
B_1 (in μm)	0.068 404 3
B_2 (in μm)	9.896 161
B_3 (in μm)	0.116 241 4

are determined experimentally by measuring spectral variation in a material. Table I enlists the numeric values of Sellmeier coefficients for silica. Equation (3) is valid for the wavelength lying between 0.21 and 2.2 μm. Depending upon the requirements, high-index glass materials such as chalcogenide glass can also be considered as a bulk glass substrate. As a matter of fact, chalcogenide glass can be better as compared to other glasses in terms of their higher thermal stability and better chemical reactivity.[9] The refractive index of these glasses is comparatively high (>2) as compared to normal glass (such as fused silica). The refractive index of chalcogenide materials is also wavelength dependent. For instance, the so-called 2S2G chalcogenide glass (i.e., $Ge_{20}Ga_5Sb_{10}S_{65}$) has following expression for its wavelength-dependent refractive index,[10]

$$n_{2S2G}(\lambda) = 2.24047 + \frac{2.693 \times 10^{-2}}{\lambda^2} + \frac{8.08 \times 10^{-3}}{\lambda^4}. \quad (4)$$

In the above expression, wavelength (λ) is in μm.

B. Metal layer

In Fig. 1(b), the base of glass substrate is shown to have been coated with thin gold layer (of thickness 50 nm). According to the free-electron Drude model, the wavelength-dependent complex dielectric function (ε_m) of any metal can be written as:

$$\varepsilon_m(\lambda) = \varepsilon_{mr} + i\varepsilon_{mi} = 1 - \frac{\lambda^2\lambda_c}{\lambda_p^2(\lambda_c + i\lambda)}. \quad (5)$$

In above expression, λ_p stands for plasma wavelength, which is defined as the wavelength corresponding to frequency of the oscillations of electron density in metal. Further, λ_c stands for collision (or damping) wavelength, which corresponds to the damping of electron density oscillations due to collisions among the electrons. For gold, the standard value of plasma wavelength (λ_p) is 168.26 nm and of collision wavelength (λ_c) is 8.93 μm.[14]

C. Buffer layer

The gold layer in Fig. 1(b) is followed by a buffer layer. However, this buffer layer has to be of different thickness depending on which glass material is used as bulk substrate. In case of 2S2G chalcogenide glass as bulk substrate, thickness of this buffer layer has to be in the vicinity of 200 nm in order to efficiently couple the incoming light due to much larger difference between n_c and n_s. In case of silica substrate, the buffer layer should have thickness in the vicinity of 1–15 nm.[15] The above ranges of buffer layer thickness are decided based on the related simulation results. Preferably, this buffer layer should be in the form of a biochemical layer due to two important reasons. First, it may contribute in preventing the blood sample from being in direct contact of metal layer which may contaminate the blood sample thereby affecting its detection accuracy. Second, the structural compatibility of blood sample with such a bio-layer is another added advantage. Due to above two reasons, the refractive index of buffer layer is set at 1.45 for both silica and 2S2G substrates for further discussion.

D. Blood sample layer

The final layer in the present SPR sensor configuration is sensing medium, which is a very thin layer of blood sample to be detected. It is worth-mentioning here that in case of SPR sensors, a very small amount (generally a few tiny drops) of sensing medium sample (i.e., blood in the present case) is required due to very high optical activity of plasmons.

E. Sensing procedure

In Fig. 1(b), *p*-polarized light from a source at a particular wavelength is incident at the substrate-metal interface and the light reflected from such multilayer system is collected by a detector. In Fig. 1(b), incident light is labeled as IL whereas reflected light is labeled as RL. Usually highly precise angular detectors of typical resolutions of the order of 0.01° or even 0.001° are available. As shown in Fig. 1(b), the information about reflected light is the only measure of SPR-based detection. Therefore, the value of reflectivity (R_p) should be observed with as much precision as possible in order to avoid any errors in recording the resonance angle (θ_{SPR}), which finally gives us the whole information of sensing medium [see Eq. (1)]. For this purpose, we have used the Transfer matrix method for multilayer system in order to obtain the expression for reflectivity of *p*-polarized incident beam.[15] The matrix method is very accurate as it contains no approximations. A detailed description of matrix method in terms of multilayer structure used in the present sensor scheme has been given in Appendix.

III. RESULTS AND DISCUSSION

In this section, we present and discuss the simulation results, which show that the precise and simple blood-group detection is surely possible with the present SPR-based sensor model.

A. Possibility of light coupling and SPR

Figure 2(a) shows the variation in refractive index of fused silica substrate [according to Eq. (3)] and 2S2G chalcogenide substrate [according to Eq. (4)] with wavelength. In Fig. 2(a), variation in "average" refractive index of human blood experimentally observed by Li *et al.* [i.e., according to Eq. (2)] is also plotted. These curves are plotted together to

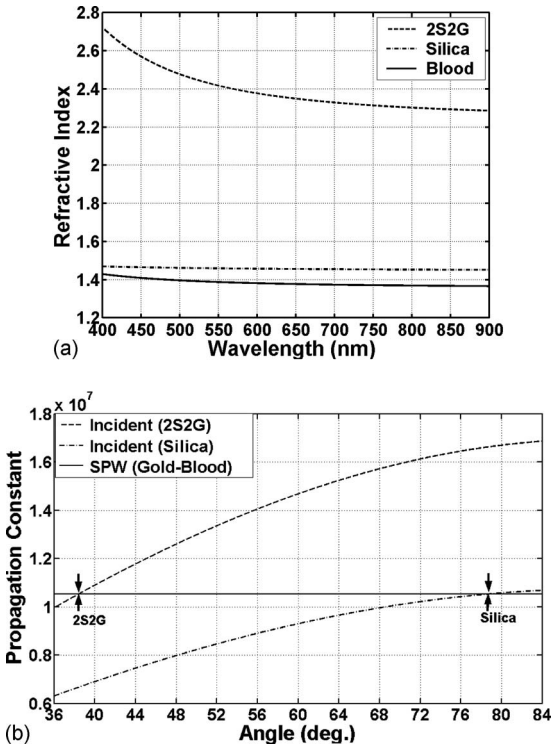

FIG. 2. (a) Variation in refractive indices with wavelength for fused silica, 2S2G chalcogenide, and average blood sample. (b) Ilustration of matching of plasmon resonance condition in case of average blood sample. The value of propagation constant is shown in m^{-1}. Separate matching is shown for fused silica and 2S2G.

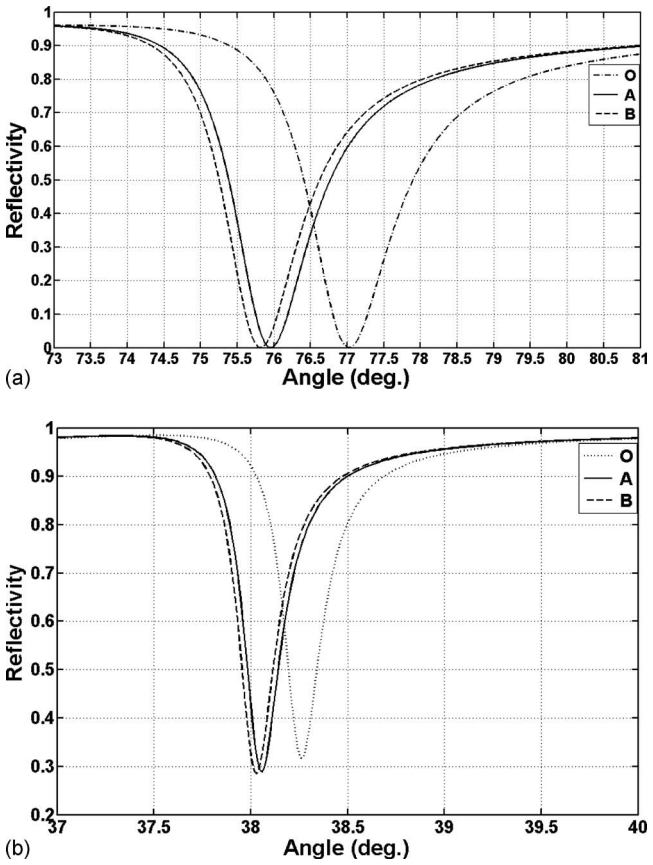

FIG. 3. Simulated SPR curves for O, A, and B blood groups corresponding to experimental dispersion data at an operating wavelength of 850 nm. The curves are separately plotted for (a) fused silica substrate and (b) 2S2G chalcogenide substrate.

analyze whether or not the foremost requirement (i.e., $n_s < n_c$) for realization of SPR is fulfilled. Here, the refractive index variations for silica and 2S2G corresponds to n_c. Whereas, the variation in blood refractive index corresponds to n_s. The wavelength range is taken as 400–900 nm because experimental data corresponding to blood refractive index was available only in this range.[13] As is visible, the value of n_c (for both silica and 2S2G) is always greater than blood refractive index n_s, which suggests that light in this wavelength range can be coupled to surface plasmons to enable SPR-based detection of blood groups. Furthermore, the difference between refractive index of silica substrate and blood sample increases for longer wavelengths, which suggests that it is better to operate at higher wavelengths (such as >850 nm) rather than at smaller wavelengths (such as 400–500 nm) in order to ensure sufficient coupling of incident light with surface plasmons. In this view, we chose the operating wavelength as 850 nm for further calculations.

Next in this sequence is to check whether or not the SPR is possible in the present scheme. The most efficient way to check this aspect is to graphically observe whether or not the plasmon resonance condition [see Eq. (1)] in the present scheme is satisfied. Figure 2(b) depicts how the propagation constants (K_{inc}) for two different substrates (i.e., silica and 2S2G) along with SPW propagation constant (K_{SP}) for blood sample vary with angle of incidence (θ). Equations (1)–(4) are used for the calculations at a wavelength (λ) of 850 nm. The intersection of the curves corresponding to K_{inc} and K_{SP} represents the fulfillment of plasmon resonance condition. As is visible, there are two different angle values (one each for silica and 2S2G substrates) where resonance condition is satisfied for the same blood sample. Two different points where resonance condition is fulfilled for silica and 2S2G have been clearly shown in the Fig. 2(b) with the help of two oppositely-directed arrows. Figure 2(b) implies that if 2S2G substrate is used then the resonance takes place at a smaller angle value (θ_{SPR}) in comparison to when silica substrate is used. Thus, above observations clarify that light coupling as well as plasmon resonance is rationally possible with the present scheme for blood-group detection.

B. Blood-group detection: Silica substrate

Figure 3(a) shows three SPR curves for three different blood groups (O, A, and B) with fused silica as the substrate material. The curves have been simulated for average dispersion data, i.e., variation in refractive index (n_s) with wavelength, corresponding to all three blood groups. The average dispersion data was obtained by taking an average of the experimental data presented by Li *et al.*[13] In their work, Li *et al.*[13] presented the experimental dispersion curves for three samples per blood group. The dispersion curves corresponding to three samples (for each blood group) were found to be substantially close to one another. For instance, three samples for A-group were having their respective dispersion curves in a very close vicinity to one another. The same trend was observed for other two blood groups as well. Therefore,

instead of separately taking each sample per blood group, it may be preferable to average-out the three dispersion curves for each blood group. Therefore, a precise averaging of experimental dispersion data was done separately at all wavelengths for each blood group's three different samples. Consequently, we got one each average dispersion curve for all three blood groups. According to Fig. 3(a), the resonance angle (θ_{SPR}) values for O, A, and B-groups are 77.03°, 75.96°, and 75.82°, respectively. The above resonance angle values are fairly separated from one another exhibiting an overall shift in resonance angle of 1.21° for three blood groups. Keeping in mind that an angular shift of as small as 0.01° is very commonly detectable with most of the modern detectors, the above results indicate that it can indeed be possible to perform blood-group detection with SPR-based sensor.

However, as was previously mentioned that apart from shift in resonance angle (i.e., sensitivity aspect), the performance of any SPR sensor heavily depends on the width (i.e., FWHM) of the resonance curve. If the curve is too broad, then the error in measuring θ_{SPR} will also be large, which will directly affect the precision with which the detection of blood group is carried out. Therefore, it is very important to investigate the width-related (i.e., accuracy) aspect of the present sensor. According to Fig. 3(a), the FWHM values for O, A, and B blood groups are 1.45°, 1.35°, and 1.34°, respectively. So, as a next step, it is necessary to evaluate whether or not the above-mentioned angular shift and FWHM of SPR curves to be used for detecting different blood groups can be further improved. For this purpose, we evaluate the performance of present sensor model by replacing fused silica with 2S2G chalcogenide substrate.

C. Performance evaluation: 2S2G substrate

Figure 3(b) depicts three SPR curves for three different blood groups (O, A, and B) with 2S2G chalcogenide as the substrate material. Similar to Fig. 3(a), the curves in Fig. 3(b) also correspond to the average dispersion of all the three blood groups (as explained in last section). According to Fig. 3(b), the resonance angle (θ_{SPR}) values for O, A, and B groups are 38.26°, 38.06°, and 38.03°, respectively. The overall shift in resonance angle for three blood groups is 0.23°, which is much smaller than that in case of fused silica substrate material (i.e., 1.21°). To be more elaborative, overall shift is more than five times larger when silica substrate (and not 2S2G) is used. As far as the SPR curve width in Fig. 3(b) is concerned, the FWHM values for O, A, and B blood groups are 0.16°, 0.15°, and 0.14°, respectively. This is a very crucial observation as the above FWHM values are at least nine times lesser than those in case of fused silica substrate (i.e., 1.45°, 1.35°, and 1.34°, respectively). The results suggest that there can be as large as ninefold (i.e., almost one magnitude) enhancement in detection accuracy of the sensor if fused silica is replaced with 2S2G chalcogenide substrate. However, this accuracy enhancement can only be brought at the cost of a fivefold decrease in overall angular shift corresponding to three blood groups, as discussed above. Consequently, there is a trade-off between silica and 2S2G substrates in terms of their respective angular shift and FWHM. Fused silica can provide a high angular shift but not so sharp SPR curve. The reverse is true for 2S2G chalcogenide material. The bottom line in this trade-off is that if a detector with a resolution of 0.001° can be used, then 2S2G chalcogenide substrate can be a preferred candidate because in that case an overall shift of 0.23° will be easily detectable as well as practically sufficient in order to reliably differentiate among the three blood groups. Moreover, the blood-group detection accuracy will be at least nine times better than fused silica as described earlier. However, if a detector of only 0.01° is used then fused silica should be chosen as substrate material because an overall shift of 1.21° may be capable of comfortably differentiating among the three blood groups. Moreover, this angular shift may also be large enough to compensate for any error occurring due to broader SPR curves.

D. Effect of imaginary part of blood refractive index

Due to nonavailability of imaginary part of blood refractive index (n_s) in the reported literatures, we could only consider the real part of n_s. The imaginary part of sensing medium refractive index is, in principle, responsible for an improvement in SPR sensor's detection performance. The reason behind this possible improvement is a corresponding variation in the SPW propagation constant (K_{SP}). Due to sensing medium being absorbing (i.e., n_s having an imaginary part) K_{SP} will increase, which will eventually make the SPR curve sharper than that when the sensing medium is nonabsorbing. It suggests that the FWHM of SPR curve becomes further smaller than we have reported in the above results, which should make the proposed SPR-based blood-group detection more accurate.

Further, it is also important to mention the effect of this imaginary part on overall shift (in θ_{SPR}) in SPR curve in the present study. It is a well-established principle among the SPR-related research studies that overall shift and FWHM of SPR curve are driven mainly, respectively, by the real and imaginary parts of K_{SP}. So, an imaginary part of blood refractive index should also affect the real part of K_{SP}, and hence, the overall shift in SPR curve. However, it has been found in several SPR sensor studies that variation in absorption by SPR-active region primarily affects the FWHM of SPR curve and does not make much effect on shift in SPR curve. Therefore, imaginary part of blood refractive index should better the sensor's performance in terms of decreased FWHM (as explained above in this section) along with not much effect on overall shift in SPR curve. Furthermore, having a prior estimation related to spectral variation in imaginary part of blood refractive index can enable to calculate an optimized thickness of gold layer in order to tune the overall shift in SPR curve toward the maximum value.

IV. CONCLUSION

A detailed analysis of SPR phenomenon in human blood-group detection is carried out with an emphasis on achieving sufficient angular shift and high detection accuracy. The different blood groups of human can indeed be differentiated by using a very efficient, easy and accurate

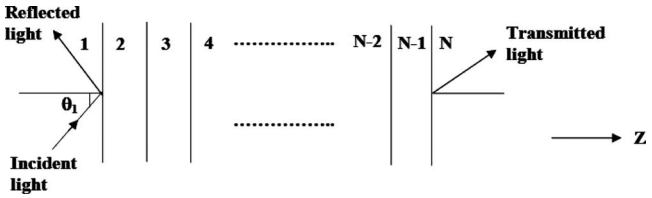

FIG. 4. Ilustration of transfer matrix model for calculating reflectivity of the present optical system.

method of SPR detection with silica or chalcogenide glass material in near IR region. It is established that by merely using a detector having a resolution of 0.001°, 2S2G chalcogenide material can be opted as a preferred substrate in order to achieve reasonable angular detection of blood groups with very high accuracy. In case of lower-resolution detectors, silica is a preferred substrate. Since the calculations have been carried out using experimental data, therefore, proposed sensor can be really helpful for blood-group detection in medical application requiring only a small amount of blood.

Blood-group detection in patients and donors is of utmost importance in transfusion medicine. Transfusion of mismatched blood groups to patients can cause fatal inflammatory and hemolytic reactions.[16] It is also a critical measurement in other medical contexts such as chirurgy involving tested blood infusions. Recently, in two different studies, the linkage of blood-group information with the risk of pancreatic cancer[17] and malaria[18] has been highlighted. The other known applications of blood-group detection can be organ transplants, paternity testing, and genetic linkage testing. Knowing the importance of blood detection in different medical contexts, the proposed sensor, apart from differentiating the different blood groups, can open up new ways for simpler, faster, and more reliable detection of overall blood properties. For instance, among others, sugar level in blood (i.e., diabetes), viruses of different diseases, and level of variable contaminants in blood.

ACKNOWLEDGMENTS

We are grateful to all our colleagues for several positive discussions and suggestions. All the authors have made equal contribution in this article.

APPENDIX: DESCRIPTION OF TRANSFER MATRIX METHOD

Since the present structure is a multilayer one (i.e., substrate-gold layer-buffer layer-sensing layer), so we have used the transfer matrix method for n-layer model in order to obtain the expression for amplitude reflection coefficient for p-polarized incident beam. The matrix method is very accurate as it contains no approximations. The layers are assumed to be stacked along the z-axis (see Fig. 4). The arbitrary medium layer is defined by thickness d_k, dielectric constant ε_k, permeability μ_k, and refractive index n_k. The tangential fields at the first boundary $Z=Z_1=0$ are related to those at the final boundary $Z=Z_{N-1}$ by

$$\begin{bmatrix} U_1 \\ V_1 \end{bmatrix} = M \begin{bmatrix} U_{N-1} \\ V_{N-1} \end{bmatrix}, \tag{A1}$$

where U_1 and V_1, respectively, are the tangential components of electric and magnetic fields at the boundary of first layer. U_{N-1} and V_{N-1} are the corresponding fields at the boundary of N_{th} layer. Here, M is known as characteristic matrix of the combined structure and is given by

$$M = \prod_{k=2}^{N-1} M_k = \begin{bmatrix} M_{11} & M_{12} \\ M_{21} & M_{22} \end{bmatrix}, \tag{A2}$$

with

$$M_k = \begin{bmatrix} \cos\beta_k & (-i\sin\beta_k)/q_k \\ -iq_k\sin\beta_k & \cos\beta_k \end{bmatrix}, \tag{A3}$$

where

$$q_k = \left(\frac{\mu_k}{\varepsilon_k}\right)^{1/2} \cos\theta_k = \frac{(\varepsilon_k - n_1^2\sin^2\theta_1)^{1/2}}{\varepsilon_k}, \tag{A4}$$

and

$$\beta_k = \frac{2\pi}{\lambda} n_k \cos\theta_k (z_k - z_{k-1}) = \frac{2\pi d_k}{\lambda}(\varepsilon_k - n_1^2\sin^2\theta_1)^{1/2}. \tag{A5}$$

In the present model, there are four layers, hence N=4. Therefore, accordingly, n_1 is the refractive index of substrate material (calculated from: Eq. (3) for silica and Eq. (4) for 2S2G), $n_2(=\sqrt{\varepsilon_m})$ is the refractive index of gold layer [calculated from Eq. (5)], n_3 is the refractive index of buffer layer (taken as 1.45), and n_4 is the refractive index of sensing layer (i.e., blood sample, calculated from experimental data for different blood groups). The dielectric constant and refractive index are related according to $n_k=\sqrt{\varepsilon_k}$ for each layer. Thus, transfer matrices M_2 (for second layer, i.e., gold layer) and M_3 (for third layer, i.e., buffer layer) are calculated in accordance with Eqs. (A3)–(A5). For these calculations, parameter d_k is the thickness of concerned layer. For gold layer, this parameter is $d_2=50$ nm. For buffer layer, this parameter is either $d_3=200$ nm (for 2S2G substrate) or $d_3=0$ (for silica substrate). The parameter θ_1 is the incident angle at the prism base (in radians). For the present study, θ_1 is varied between 72° (i.e., 1.256 rad) and 84° (i.e., 1.465 rad) for silica substrate. Whereas, for 2S2G substrate, θ_1 is varied between 37° (i.e., 0.645 rad) and 40° (i.e., 0.698 rad). The parameter λ is the light wavelength, which is taken as 850 nm for the present analysis. These two matrices are multiplied to obtain the final transfer matrix M of the present multilayer setup [see Eq. (A2)]. With this 2×2 matrix M, it's four elements M_{11}, M_{12}, M_{13}, and M_{14} are obtained [see Eq. (A2)]. These four elements are used to calculate the amplitude reflection coefficient (r_p) for p-polarized incident wave as follows:

$$r_p = \frac{(M_{11} + M_{12}q_4)q_1 - (M_{21} + M_{22}q_4)}{(M_{11} + M_{12}q_4)q_1 + (M_{21} + M_{22}q_4)}. \tag{A6}$$

In the Eq. (A6), q_1 is the corresponding term for substrate and q_4 is the corresponding term for sensing layer. Both these terms are calculated from Eq. (A4) by putting

their corresponding refractive index values (i.e., n_1 and n_4), dielectric constants (i.e., ε_1 and ε_4), and incident angle values. Finally, reflectivity (R_p) for p-polarized light is

$$R_p = |r_p|^2. \tag{A7}$$

[1]Z. Salamon, H. A. Macleod, and G. Tollin, Biochim. Biophys. Acta **1331**, 117 (1997).
[2]E. Matveeva, J. Malicka, I. Gryczynski, Z. Gryczynski, and J. R. Lacowicz, Biochem. Biophys. Res. Commun. **313**, 721 (2004).
[3]Rajan, S. Chand, and B. D. Gupta, Sens. Actuators B **123**, 661 (2007).
[4]W. B. Lin, M. Lacroix, J. M. Chovelon, N. Jaffrezic-Renault, and H. Gagnaire, Sens. Actuators B **75**, 203 (2001).
[5]A. K. Sharma and B. D. Gupta, Opt. Fiber Technol. **12**, 87 (2006).
[6]R. C. Jorgenson and S. S. Yee, Sens. Actuators B **12**, 213 (1993).
[7]S. Patskovsky, A. V. Kabashin, M. Meunier, and J. H. T. Luong, Sens. Actuators B **97**, 409 (2004).
[8]E. Kretschmann and H. Reather, Z. Naturforsch. A **23A**, 2135 (1968).
[9]B. Bureau, X. H. Zhang, F. Smektala, J. Adam, J. Troles, H. Ma, C. Boussard-Pledel, J. Lucas, P. Lucas, D. Le Coq, M. R. Riley, and J. H. Simmons, J. Non-Cryst. Solids **345** and 346, 276 (2004).
[10]J. Le Person, F. Colas, C. Compere, M. Lehaitre, M. Anne, C. Boussard-Pledel, B. Bureau, J. Adam, S. Deputier, and M. Guilloux-Viry, Sens. Actuators B **130**, 771 (2008).
[11]R. Jha, and A. K. Sharma, J. Opt. A, Pure Appl. Opt. **11**, 045502 (2009).
[12]R. Jha and A. K. Sharma, Opt. Lett. **34**, 749 (2009).
[13]H. Li, L. Lin, and S. Xie, Proc. SPIE **3914**, 517 (2000).
[14]J. Homola, Sens. Actuators B **41**, 207 (1997).
[15]B. D. Gupta and A. K. Sharma, Sens. Actuators B **107**, 40 (2005).
[16]P. Palacajornsuk, C. Halter, V. Isakova, M. Tarnawski, J. Farmar, M. E. Reid, and A. Chaudhuri, Transfusion (Paris) **49**, 740 (2009).
[17]B. M. Wolpin, A. T. Chan, P. Hartge, S. J. Chanock, P. Kraft, D. J. Hunter, E. L. Giovannucci, and C. S. Fuchs, J. Natl. Cancer Inst. **101**, 424 (2009).
[18]J. A. Rowe, D. H. Opi, and T. N. Williams, Curr. Opin. Hematol. **16**, 480 (2009).